EUROfusion

WPMAG-CPR(17) 17870

A. Dembkowska et al.

Thermal-Hydraulic Analysis of the DEMO CS coil

Preprint of Paper to be submitted for publication in Proceeding of
13th European Conference on Applied Superconductivity

This work has been carried out within the framework of the EUROfusion Consortium and has received funding from the Euratom research and training programme 2014-2018 under grant agreement No 633053. The views and opinions expressed herein do not necessarily reflect those of the European Commission.

Thermal-Hydraulic Analysis of the DEMO CS coil

Aleksandra Dembkowska, Monika Lewandowska, Xabier Sarasola

***Abstract*— Two alternative designs of the Central Solenoid (CS) coil were proposed by EPFL-SPC PSI Villigen and CEA Cadarache for the European DEMO tokamak. The DEMO CS coil consists of five modules, namely CSU3, CSU2, CS1, CSL2 and CSL3, the most demanding of which is the CS1 one. Our present work is focused on the thermal-hydraulic analysis of the CS1 module designed by EPFL-SPC at the normal operating conditions during the whole current cycle. We took into account the realistic magnetic field distribution, heat transfer between neighboring turns, and heat generation due to AC losses. The analysis, performed using the THEA Cryosoft code, was aimed at the assessment of the minimum temperature margin and at verification if the proposed design fulfills the acceptance criteria. For the considered current scenario the minimum of the temperature margin was observed at the end of the dwell phase. The temperature margin in the sub-coils 1-9 was above the 1.5 K criterion, but was slightly too small in the most outer sub-coil 10.**

***Index Terms*— DEMO CS coil, CS1 module, thermal-hydraulic analysis, temperature margin.**

I. Introduction

CONCEPTUAL studies on the European DEMOnstration Fusion Reactor (DEMO), designed to demonstrate at the middle of this century feasibility of net electricity production at the level of a few hundred MW, are carried out under the lead of the EUROfusion Consortium [1]-[3]. The core of DEMO will be a tokamak with a superconducting magnet system. A large part of the previous design and assessment studies carried out by the DEMO Magnet System project team was focused on the Toroidal Field (TF) coils, but in 2015 the work on the Central Solenoid (CS) design was also initiated [4], [5]. According to the 2015 DEMO reference, the DEMO CS coil will consist of five modules, namely CSU3, CSU2, CS1, CSL2 and CSL3, positioned vertically one above the other [6]. The central CS1 module will operate under the most demanding conditions, i.e. the highest magnetic fields and mechanical loads. Recently two alternative designs of the DEMO CS1 modules have been proposed by EPFL-SPC, PSI Villigen and CEA Cadarache [7]-[9]. Our present work is focused on the thermal-hydraulic analysis of the CS1 module, designed by EPFL-SPC, aimed at the assessment of the minimum temperature margin at the normal operating conditions and at verification if the proposed design fulfills the acceptance criteria.

This work was carried out within the framework of the EUROfusion Consortium and was supported in part by the Euratom Research and Training Program 2014–2018 under Grant 633053 and in part by the Polish Ministry of Science and Higher Education within the framework of the financial resources in the year 2017 allocated for the realization of the international cofinanced project. (*Corresponding author: M. Lewandowska*)

A. Dembkowska and M. Lewandowska are with the West Pomeranian University of Technology, Szczecin, 70-310 Szczecin, Poland (e-mail: monika.lewandowska@zut.edu.pl).

X. Sarasola is with EPFL/SPC, 5232 Villigen PSI, Switzerland

II. Model Assumptions

The design of the CS1 module proposed in [7] was subjected to FEM mechanical analyses which resulted in its further improvements, as described in details in [8]. Our analysis is based on the last, 3rd, iteration of the design presented in [8]. The EPFL-SCP CS1 design is based on a layer-wound concept with superconductor grading. The winding pack is composed of 10 sub-coils (SC), each consisting of 2 layers wound with cables of the same kind. The 2 most inner SC, located in a high magnetic field, use Re-123 High T_c Superconductor (HTS), the next 5 SC in the medium magnetic field region are made of R&W Nb_3Sn conductors, and the 3 most outer SC in the low field utilize NbTi. Schematic layout of HTS and Low T_c Superconductor (LTS) cables designed for the CS1 coil is presented in Fig. 1, and their characteristics relevant for the present analysis is given in Table I. In the 2nd column of Table I lengths of the shorter conductor in each SC, subjected to the higher magnetic field, is shown. In Table I A is the component cross section, φ is the effective void fraction, and D_h is the hydraulic diameter. Indices *hast*, *B*, *scon* denote hastelloy, bundle and superconductor, respectively. Index *side* refers to two side channels. We assume that copper in HTS tapes has RRR = 53, in LTS strands (index *Cu*1), in the outer part of strands and in cores of HTS conductors has RRR = 100, whereas copper in segregated strands (index *Cu*2) and in the outer stabilizer (index *stab*) of LTS conductors is characterized by RRR = 400. We assume that the superconductors' properties are characterized by the scaling laws specified in [7].

The assumed plasma scenario includes 10 s premagnetisation (P), 80 s breakdown, 120 min burn (between the Start of Flat Top (SOF) and the End of Flat Top (EOF)) and 10 min dwell phases [3],[9]. The corresponding current scenario is presented in Fig. 2. The maximum value of the operating current is I_P = 51.22 kA [8], whereas the ratio of the currents at the characteristic points of the current cycle is assumed to be $I_P : I_{SOF} : I_{EOF}$ = 57.14 : -8.79 : -57.14 [11].

The profiles of the radial and vertical component of the

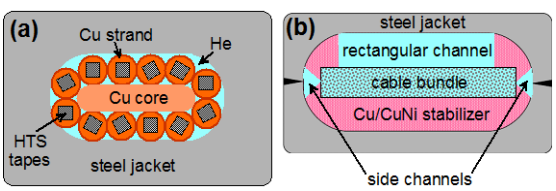

Fig. 1. Schematic layout of a (a) HTS, (b) LTS cable.

TABLE I
CONDUCTORS PARAMETERS USED IN THE PRESENT ANALYSIS. THE COMPLETE CONDUCTORS CHARACTERISTICS CAN BE FOUND IN [8].

HTS SC	L (m)	A_{scon} (mm^2)	A_{hast} (mm^2)	$A_{Cu\ Tapes}$ (mm^2)	A_{Ag} (mm^2)	$A_{Cu\ Strands}$ (mm^2)	A_{core} (mm^2)	A_{He} (mm^2)	D_h (mm)	A_{jacket} (mm^2)
1	972.4	1.89	94.6	75.7	7.19	188.7	188.7	151.2	1.52	2862.1
2	999.8	1.73	86.4	69.1	6.57	206.0	206.0	141.0	1.40	2817.9

LTS SC	L (m)	A_{scon} (mm^2)	$A_{Cu1\ B}$ (mm^2)	$A_{Cu2\ B}$ (mm^2)	$A_{He\ B}$ (mm^2)	$D_{h\ B}$ (mm)	φ (-)	$A_{He\ side}$ (mm^2)	$D_{h\ side}$ (mm)	$A_{He\ rect}$ (mm^2)	$D_{h\ rect}$ (mm)	A_{stab} (mm^2)	A_{jacket} (mm^2)
3	1054	109.2	109.2	12.1	79.7	0.531	0.250	41.9	2.01	112.3	12.78	305.5	2727.4
4	1105	71.8	71.8	8.0	52.3	0.452	0.250	70.6	2.78	95.0	11.85	350.7	2589.7
5	1155	50.0	50.0	16.7	40.9	0.481	0.250	37.1	1.94	130.4	13.75	362.3	2509.1
6	1203	35.7	35.7	11.9	29.3	0.412	0.250	44.2	1.90	128.7	13.70	382.9	2455.7
7	1250	26.0	26.0	8.7	21.3	0.397	0.249	56.3	1.93	120.4	13.30	397.4	2420.0
8	1298	84.8	84.8	9.4	61.71	0.490	0.250	66.8	2.75	99.29	12.19	345.6	2675.9
9	1348	29.2	29.2	9.7	23.89	0.419	0.250	57.4	2.02	118.71	13.21	394.1	2436.9
10	1394	15.5	15.5	5.2	12.14	0.372	0.248	62.2	1.76	118.84	13.26	412.4	2383.1

magnetic field along each conductor, $B_r(x)$ and $B_z(x)$, taking into account contributions generated by all the CS modules as well as the Poloidal Field coils, were computed for the characteristic points of the cycle using the 2D axi-symmetrical finite element model in ANSYS. By linear interpolation of these data we obtained the values of $B_r(x,t)$ and $B_z(x,t)$ and finally we computed the magnetic field magnitude $B(x,t)=(B_r^2(x,t)+B_z^2(x,t))^{1/2}$. Examples of the magnetic field evolution during the breakdown phase are shown in Figs. 3.

Fig. 2. The considered current scenario.

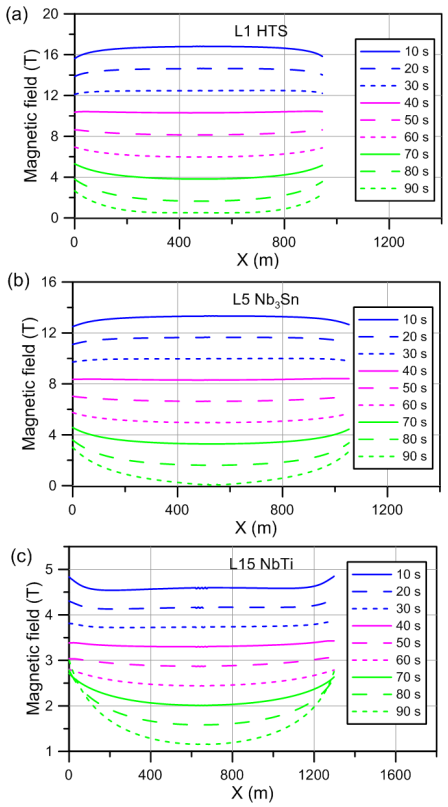

Fig. 3. The computed magnetic field profile evolution in the layers (a) L1, (b) L5, and (c) L15 during the breakdown phase.

The AC coupling loss per unit length of conductor in a field ramped at a uniform rate $\dot{\vec{B}}$ is calculated as [11]:

$$P_{coupling}(x)=\frac{n\tau S}{\mu_0}\left(\frac{d\vec{B}(x)}{dt}\right)^2=\frac{n\tau S}{\mu_0}\left[\left(\frac{dB_r(x)}{dt}\right)^2+\left(\frac{dB_z(x)}{dt}\right)^2\right], \quad (1)$$

where n is the shape factor, τ is a time constant dependent on the conductor parameters, and S is the conductor cross section (excluding helium and steel jacket), respectively. As agreed with the project team, to assess coupling losses in the DEMO CS conductors we use the $n\cdot\tau = 75$ ms taken from the ITER DDD [12]. The values of $\dot{B}_r(x)$ and $\dot{B}_z(x)$ during the breakdown, burn and dwell phases were estimated using the respective $B_r(x)$ and $B_z(x)$ values at the beginning and end of the given phase, e.g.

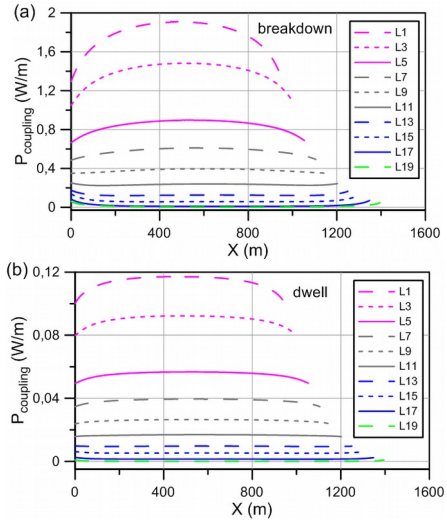

Fig. 4. The computed AC losses distribution along the CS1 conductors during (a) the breakdown phase, (b) the dwell phase.

$$\dot{B}_i(x)_{breakdown} \approx \left[B_i(x)_{SOF} - B_i(x)_P\right]/80 \text{ s}, \qquad i = r, z. \tag{2}$$

The resulting $P_{coupling}$ profiles in different layers during the breakdown and dwell phases are presented in Figs. 4. The $P_{coupling}$ values during the burn phase are much smaller, in the range 10^{-5} - $2 \cdot 10^{-4}$ W/m.

As in previous studies of the DEMO TF coil, e.g. [13]-[17], we assume that cooling conditions of the DEMO CS coil are similar to those of ITER, namely the coil is cooled by a forced flow of supercritical helium with T_{in} = 4.5 K and p_{in} = 0.6 MPa at the inlet, and the expected value of pressure drop in each conductor is 0.1 MPa. All the conductors are connected hydraulically in parallel.

The behavior of each conductor during the whole current cycle is simulated using the Cryosoft code THEA [18]-[19]. Each of conductors is modeled as the system of several parallel 1-D components, as shown schematically in Figs. 5. In the LTS cables we allowed helium exchange between the rectangular and side channels, since it is expected that the boundary between the Cu/CuNi stabilizer and the steel conduit is not tight. We conservatively assume that the heat transfer coefficient between the solid components (h) is equal to 500 W/(m^{2}K) [20], whereas the heat transfer between the solid and the fluid components is governed by the standard smooth tube correlations (h_{st}). We also take into account the inter-turn heat transfer. For the flow in the bundle regions of LTS conductors we assume the friction factor correlation based on the porous medium Darcy – Forchheimer equation [21], whereas for all the cooling channels the smooth tube the Bhatti - Shah correlation [22] is used. All the above assumptions are consistent with those made in earlier analyses of the DEMO LTS TF coils [13]-[17]. As suggested in [23], for the flow in HTS conductors we use the Fanning friction factor correlation developed for the EURATOM LCT conductor [24]:

$$f_{LCT}(\mathrm{Re}) = \frac{1}{4} \cdot \begin{cases} 47.65 \cdot \mathrm{Re}^{-0.885} & \text{for } \mathrm{Re} < 1500 \\ 1.093 \cdot \mathrm{Re}^{-0.338} & \text{for } 1500 < \mathrm{Re} < 2 \cdot 10^5 \\ 0.0377 & \text{for } \mathrm{Re} > 2 \cdot 10^5 \end{cases} \tag{3}$$

We assume the adiabatic and fixed pressure (infinite

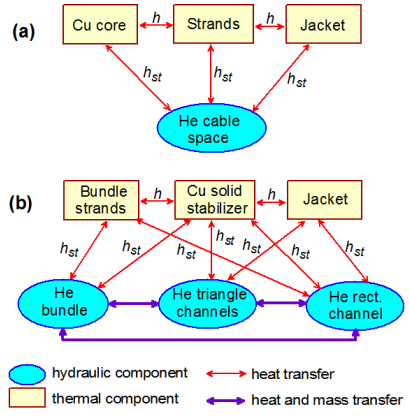

I.

II. Fig. 5. THEA model of a (a) HTS conductor, (b) LTS

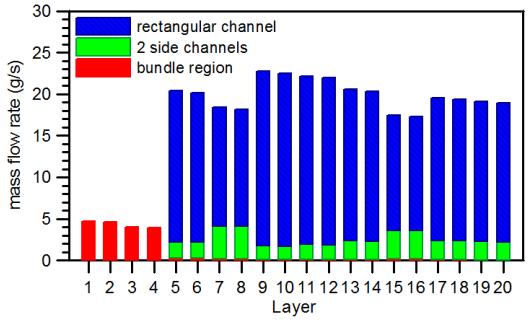

Fig. 6. Mass flow rates in each conductor of the CS1 coil assuming no heat deposition in conductors.

III. Results and Discussion

As the initial stage of our study, the hydraulic analysis of all conductors was performed. We calculated the maximum mass flow rate in each channel of flow assuming non-compressible isenthalpic flow, as in [13],[14], and using the friction correlations mentioned in Section II. The results of these calculations are shown in Fig. 6. It is seen that the mass flow rates in rectangular channels of LTS conductors is very large, whereas in the bundle regions is negligible small. Mass flow rates in HTS conductors are about 4 times smaller than in LTS conductors. It should be noted that no cables very similar to the HTS cables of the CS1 coil have been tested for pressure drop yet, so the accuracy of the f_{LCT} correlation is uncertain. The maximum total mass flow rate in the CS1 coil was assessed to be 337 g/s, which can serve as a reference for designers of the DEMO cryogenic system.

As the next stage, behaviour of the shorter conductor in each SC was studied using the THEA code. The preliminary simulations were performed assuming no heat load and with the current and the magnetic field profiles set equal to their values in the premagnetisation phase. These simulations started from the constant initial conditions $T(x) = T_{in}$, $p(x) = p_{in}$ and were carried out until the steady state was reached. We checked that the steady state mass flow rates obtained with THEA agreed well with those resulting from the hydraulic model, as expected. The stationary temperature, pressure and mass flow rate profiles along each cable were saved and later served as the initial states for the subsequent simulations of the whole current cycle, aimed at the assessment of the minimum value of the temperature margin for each of the considered conductors. The temperature margin is defined as:

$$\Delta T_{marg}(x,t) = T_{cs}(x,t) - T_{scon}(x,t), \tag{4}$$

where T_{cs} is the current sharing temperature.

The value of the temperature margin in CS1 conductors is affected by two factors: temperature rise in conductors due to the AC losses heat generation and changes of T_{cs} caused by

variations of the magnetic field and operating current. Some typical examples of the time evolution of the temperature margin profile starting from the end of the premagnetisation phase (t = 10 s) till the end of the breakdown phase (t = 90 s) are presented in Figs. 7. It is seen that during the premagnetisation phase, when the magnetic field and current are maximal but there is no heat load, the temperature margin is the lowest. During the breakdown phase the temperature rise due to relatively large AC losses is mitigated by effective cooling. Simultaneously both magnetic field and operating current decrease (see Figs. 2 and 3), which results in rise of T_{cs}. The latter effect is dominant, so as a result the temperature margin values increase. The time evolution of the minimum

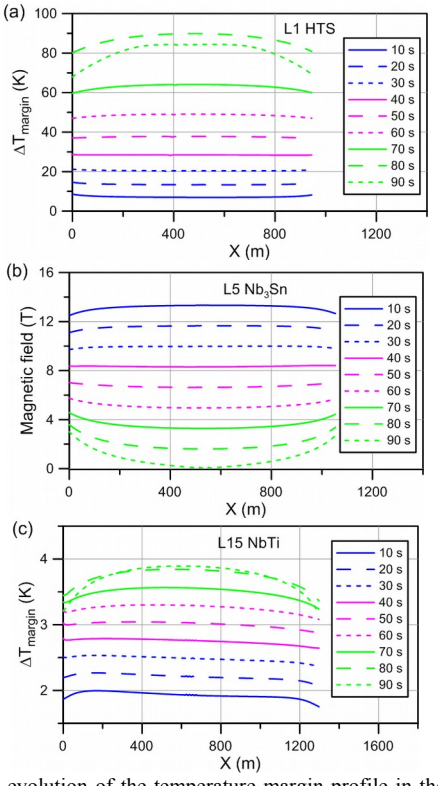

Fig. 7. Time evolution of the temperature margin profile in the layers (a)

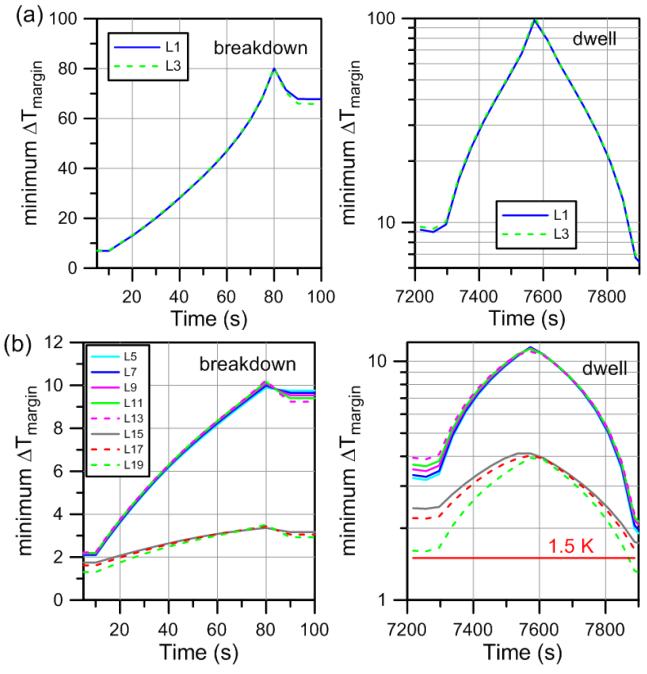

Fig. 8. Time evolution of the minimum temperature margin during the breakdown and dwell phases in the (a) HTS, (b) LTS conductors.

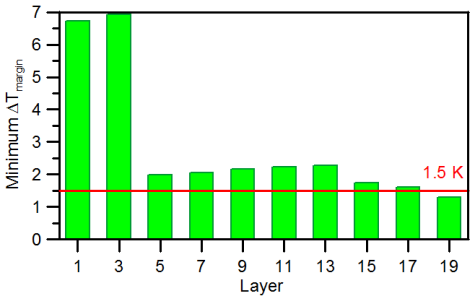

Fig. 9. Minimum temperature margin in all the considered CS1 layers.

temperature margin during the whole current cycle is shown in Figs. 8. It is seen, that in all the CS1 layers the smallest values of the temperature margin are observed in the very last seconds of the dwell phase, where they are even slightly smaller than in the premagnetisation phase, which is due to the higher conductor temperature.

The minimum values of ΔT_{marg} for all the layers and the whole current cycle are compiled in Fig. 9. It is seen that the minimum ΔT_{marg} is much larger in the HTS conductors than in the LTS conductors. For the considered current scenario the temperature margin in layers L1-L18 is above the 1.5 K acceptance criterion [25], whereas in L19 is slightly too small. This effect can be explained by the fact, that during the premagnetisation phase the computed magnetic field profile maxima, located at both ends of the L19 conductor, are about 0.5 T higher than the design peak value of the magnetic field assumed in [8] for the L19 layer.

IV. CONCLUSION

The performed hydraulic analysis of the CS1 coil (SPC design) allowed to estimate the total mass flow rate in coil equal to 337 g/s. However, predictive capability of the friction factor correlation f_{LCT} used for HTS cables should be verified experimentally.

Normal operation of the CS1 module was simulated using the THEA code during the whole plasma scenario (breakdown, burn and dwell phases). Time evolution of magnetic field profiles along the conductor, heat load due to AC coupling losses, inter-turn heat transfer and mass transfer between different channels of flow were taken into account. The evolution of the temperature margin profile in the shorter conductor of each sub-coil was simulated. For the considered current scenario the minimum value of ΔT_{marg} was typically achieved in the last seconds of the dwell phase. The computed minimum temperature margin in layers L1-L18 was sufficiently large, whereas in L19 was slightly below the 1.5 K criterion.

The obtained results should provide information for further improvements and optimization of the winding pack design.

ACKNOWLEDGMENT

The views and opinions expressed herein do not necessarily reflect those of the European Commission.

We would like to thank N. Bykovski, K. Sedlak and R. Wesche (EPFL-SPC) for providing the input data and helpful discussions.

REFERENCES

[1] "Fusion Electricity. A roadmap to the realisation of fusion energy," November 2012, Available: https://www.euro-fusion.org/wpcms/wp-content/uploads/2013/01/JG12.356-web.pdf

[2] G. Federici, *et al*., "Overview of the design approach and prioritization of R&D activities towards an EU DEMO," *Fusion Eng. Des.* 109–111 (2016) 1464–1474.

[3] G. Federici, *et al.*, "DEMO Design Activity in Europe: Progress and Updates," *Fusion Eng. Des.*, submitted for publication.

[4] L. Zani, *et al.*, "Overview of Progress on the EU DEMO Reactor Magnet System Design," *IEEE Trans. Appl. Supercond*., vol. 26, no. 4, Jun. 2016, Art. no. 4204505.

[5] R. Wesche, *et al*., "Winding pack proposal for the TF and CS coils of European DEMO," *IEEE Trans. Appl. Supercond*., vol. 26, no. 3, Apr. 2016, Art. no. 4200405.

[6] B. Meszaros, "EU DEMO1 2015 – DEMO-Tokamak-Complex," (CAD Model), 2015, https://idm.euro-fusion.org/?uid=2D3FBF .

[7] R. Wesche, N. Bykovsky, X. Sarasola, K. Sedlak, B. Stepanov, D. Uglietti, and P. Bruzzone, "Central solenoid winding pack design for DEMO," *Fusion Eng. Des.*, to be published.

[8] R. Wesche and X. Sarasola, "Report on CS Winding Pack Design and Analysis," Final report MAG-2.1-T004-D003, 2017, https://idm.euro-fusion.org/?uid=2MRPVA

[9] R. Vallcorba, B. Lacroix, D. Ciazynski, A. Torre, F. Nunio, L. Zani, Q. Le Coz, S. Nicollet, V. Corato, and M. Coleman, "Thermohydraulic Analyses on CEA Concept of TF and CS Coils for EU-DEMO," *IEEE Trans. Appl. Supercond.*, submitted for publication.

[10] R. Ambrosino and R. Albanese, "Reference flat-top equilibria for DEMO with aspect ratio 3.1," EUROfusion report, https://idm.euro-fusion.org/?uid=2AQ5GP

[11] A.M. Campbell, "A general treatment of losses in multifilamentary superconductors," *Cryogenics*, vol. 22, no. 1, pp. 3–16, Jan. 1982.

[12] ITER Design Description Document. Magnets. Section 7: Conductors, ITER_D_2NBKXY v1.2, 2009.

[13] M. Lewandowska and K. Sedlak, "Thermal-hydraulic analysis of LTS cables for the DEMO TF coil," *IEEE Trans. Appl. Supercond*., vol. 24, no. 3, Jun. 2014, Art. no. 4200305.

[14] M. Lewandowska, K. Sedlak and L. Zani, "Thermal-hydraulic analysis of the low-T_c Superconductor (LTS) winding pack design concepts for the DEMO Toroidal Field (TF) coil," *IEEE Trans. Appl. Supercond*., vol. 26, no. 4, Jun. 2016, Art. No. 4205305.

[15] R. Zanino et al., "Development of a Thermal-Hydraulic Model for the European DEMO TF Coil," IEEE Trans. Appl. Supercond., vol. 26, no. 4, Jun. 2016, Art. no. 4201606.

[16] R. Vallcorba et al., "Thermo-hydraulic analyses associated with a CEA design proposal for a DEMO TF conductor," *Cryogenics*, vol. 80, 2016, pp. 317–324.

[17] K. Sedlak, P. Bruzzone and M. Lewandowska, "Thermal-hydraulic and quench analysis of the DEMO toroidal field winding pack WP1," *Fus. Eng. Des.*, to be published.

[18] L. Bottura, C. Rosso, and M. Breschi, "A general model for thermal, hydraulic and electric analysis of superconducting cables," Cryogenics, vol. 40, no. 8–10, pp. 617–626, Aug.–Oct. 2000.

[19] THEA—Thermal, Hydraulic and Electric Analysis of Superconducting Cables. User's Guide Version 2.3, CryoSoft, Sept. 2016, Available: https://supermagnet.sourceforge.io/manuals/Thea_2.3.pdf .

[20] N. Koizumi, T. Takeuchi, and K. Okuno, "Development of advanced Nb_3Al superconductors for a fusion DEMO plant," *Nucl. Fusion*, vol. 45, no. 6, pp. 431–438, May 2005.

[21] M. Bagnasco, L. Bottura, and M. Lewandowska, "Friction factor correlation for CICC's based on a porous media analogy," *Cryogenics*, vol. 50, no. 11/12, pp. 711–719, Nov./Dec. 2010.

[22] R.K. Shah, D.P. Sekulić, *Fundamentals of Heat Exchanger Design*, Wiley, New Jersey, 2003, p. 482.

[23] R. Heller, P. V. Gade, W.H. Fietz, Senior M, T. Vogel, and K.-P.Weiss, "Conceptual Design Improvement of a Toroidal Field Coil for EU DEMO Using High-Temperature Superconductors," *IEEE Trans. Appl. Supercond.* vol. 26, no. 4, Jun. 2016, Art. no. 4201105.

[24] D. S. Beard, W. Klose, S. Shimamoto, and G. Vecsey, "The IEA largecoil task development of superconducting toroidal field magnets for fusion power," *Fusion Eng. Des.*, vol. 7, no. 1/2, pp. 1–230, 1988.

[25] L. Zani, *et al.*, "Overview of Progress on the EU DEMO Reactor Magnet System Design," *IEEE Trans. Appl. Supercond.* vol. 26, no. 4, Jun. 2016, Art. no. 4204505.